Investigating Whether the Improvement of the AMP-Activated Protein Kinase (AmpK) is Neuroprotective in Huntington's Disease Neurons

Manasa Chillarige

Huntington's disease (HD) is a hereditary condition which causes disordered movement, behavioral changes, and dementia. As with many neurological diseases, there is no effective treatment and HD is universally fatal. Metformin has been found improve cognitive score in diabetic patients with HD and has also improved motor function and decreased mutant HTT aggregates in mice brains. Like metformin, BC1618 is an inhibitor of Fbxo48. However, its potency in stimulating Ampk-dependent signaling greatly exceeds metformin. GA100 also works in a similar manner as BC1618. Thus, Q7 and Q111 cell lines were treated with 5 and 10 μM concentrations of BC1618 or GA1000 and the samples were collected to perform protein, RNA, and DNA analysis. The most significant results from this experiment came from the qPCR results which confirmed the initial hypothesis and supported the idea that both BC1618 and GA100 effectively inhibit Fbxo48 and prolong Ampk activation. We further hypothesize that this will promote mitochondrial biogenesis which can have neuroprotective effects on HD.

Investigating whether the Improvement of the AMP-activated protein kinase (AmpK) is neuroprotective in Huntington's Disease Neurons

Introduction

Huntington's disease (HD), a hereditary condition afflicting 30,000 Americans, causes disordered movement (chorea), behavioral changes, and dementia (1). As with many other neurological diseases, there is no effective treatment and HD is universally fatal. Patients present with unique combinations of these symptoms which can be managed through a variety of treatments including chorea medication, antipsychotic medication, antidepressants, mood-stabilizing drugs, as well as non-drug therapies. However, being able to target the root of the issue continues to be a challenge (14). Altered metabolism is a well-known symptom of HD, but the underlying causes are unknown. The treatment of HD patient with metformin is under intense study, since use of metformin for the treatment of type II diabetes in HD patients was surprisingly correlated with better cognitive score (2, 3). HD patients tend to develop glucose intolerance and metabolic dysregulation. Metformin modulates several metabolic pathways and can restore metabolic dysregulation associated with other diseases, including HD. Metformin does this by improving glucose uptake through gluconeogenesis suppression (13). Metformin is known to inhibit mitochondrial complex 1, ultimately inhibiting gluconeogenesis. Mechanistic studies in a mouse model of HD, the zQ175KI model, demonstrated improved motor function in treated mice, as well as decreased mutant HTT aggregates in the brain of the treated mice, as compared with vehicle treated controls (3). However, metformin is contraindicated in some patients and thus new drugs with the ability to inhibit gluconeogenesis through a mechanism separate from that of metformin represent a new therapeutic strategy in HD.

The AMP-activated protein kinase (Ampk) is a central regulator of metabolic pathways. Increasing Ampk activity has been a promising therapeutic target. Prior research has found that Ampk activation protects mouse striatal cells expressing mHtt, reducing their susceptibility to stress, with reduction of soluble mHtt levels by metformin. Ampk prevents the induction of neurodegeneration by mHtt, suggesting that Ampk can protect the brain from mHtt cytotoxicity in a living brain (12). Fbxo48 is a ubiquitin E3 ligase subunit protein that targets the active, phosphorylated Ampkα (pAmpkα) for polyubiquitylation and proteasomal degradation (4). BC1618 is an inhibitor of Fbxo48 and its potency in stimulating Ampk-dependent signaling greatly exceeds metformin (4). This compound increases the biological activity of Ampk not by stimulating the activation of Ampk, but rather by preventing activated pAmpkα from Fbxo48-mediated degradation. BC1618 has been found to promote mitochondrial fission, prolong Ampk activity, and decrease gluconeogenesis (4). Thus, this unique compound works to inhibit pAmpkα disposal. In this study, we will perform fundamental studies that lay the groundwork for BC1618 and GA100 to be developed as potential new therapeutics for HD.

Methods

Cell Lines Used: In this project, we will use STHdh^{Q111} (Q111) and STHdh^{Q7} (Q7) cells. The Q7 and Q111 cell lines represent wild type and full-length muHTT models of HD. These striatal cell lines were established from mouse knock-in embryos (5). Previous studies examined mitochondrial function and found that mitochondrial respiration was decreased in the muHTT line as was mitochondrial protein import. Furthermore, Q111 are more sensitive to temperature shift and serum deprivation (SDM conditions) than are Q7 and undergo cell death at a higher rate under these

conditions. Thus, these lines are useful in vitro models for studies of mitochondrial dysfunction and mitochondrially mediated cell death in the presence of muHTT (5).

Cell Culture: Q7 and Q111 mouse striatal cell lines that express full-length WT (polyQ7) and mutant (polyQ111) HTT were a gift from Marci MacDonald (Harvard Medical School, Boston, Massachusetts, USA), who generated these lines (57). Q7 and Q111 cells were grown in MEM culture medium with 10% FBS. Cells were sub-cultured when confluency reached 70-80%, indicating that a majority of the adherent surface of the culture vessel is covered with cultured cells. Subculturing was done by aspirating culture medium out of the dishes and adding 2 mL of 0.25% Trypsin-EDTA Solution. Once the cells had detached fully from the dish, the solution was collected in 10 mL centrifuge tubes and filled to 10 mL with fresh culture medium. Then, they were placed in the centrifuge (800 rpm) for 5 minutes, to allow for the cell pellet to form. The supernatant was then removed, and the cell pellet was suspended in 2 mL of medium and added to the new plates at the desired ratio (typically 1:10). For experiments, cells were counted using the Invitrogen Countess Automated Cell Counter. A mixture of 10 µl of Trypan Blue and 10 µl of cell suspension was added to the glass slide and the cell count was obtained. 3.0 x 10^6 Q7 or Q111 cells were plated in 10 cm cell culture dishes. After 24 hours, cells were treated with BC1618 or GA100 for 24 hours and then transferred to 37ºC non-permissive temperature for additional 24 hours. After 48 hours of total treatment samples were collected for RNA or DNA isolation.

Experimental Protocol: Five culture dishes were made for Q7 cells and five dishes for Q111 cells where the following conditions were tested: Control, 5 µM BC1618, 10 µM BC1618, 5 µM GA100, and 10 µM GA100. After 3.0 x 10^6 cells were plated in each dish, they were incubated in the 33°C incubator for 24 hours. The next day, regular medium was replaced with 10 mL of glucose-free medium and BC1618 and GA100 treatments were added to the dishes to create final concentration of 10 µM. The dishes were transferred to the 37°C incubator for 24 hours. On the following day, samples were collected. Samples were collected weekly: protein samples were collected in the first week, RNA samples in the second week, DNA samples in the third week.

Protein Lysate Preparation: To collect protein samples, cells were detached from the plate using trypsin, the solution was centrifuged (800 rpm) for 5 minutes, supernatant was removed, the cell pellet was dissolved in 400 µl of RIPA buffer, transferred into a 1.5 mL microcentrifuge tube and stored in -80°C freezer. For isolation, protein samples were taken out on ice and centrifuged at 15,000 g for 30 min. The supernatant was transferred to a new centrifuge tube and the pellet was discarded. A Bradford Assay was performed using the supernatant.

RNA Isolation, cDNA Preparation, and qPCR: RNA samples were purified and isolated using the RNeasy Kit from QIAGEN according to manufacturer protocol. Briefly, to collect RNA samples, cells were detached from the plate using trypsin, the solution was centrifuged (800 rpm) for 5 minutes, supernatant was removed, the cell pellet was dissolved in 350 µl of RLT buffer, transferred into a 1.5 mL microcentrifuge tube and stored in -80°C freezer. RNA samples were purified and isolated using the RNeasy Kit from QIAGEN. RNA quantification data was collected using the Nanodrop 1000. The RNA samples were then used to prepare cDNA by using High capacity reverse transcription kit from Thermo. To prepare cDNA from RNA, the reaction mixture was made using 13 µl of 10x Buffer, 13 µl of 10x Primers, 5.2 µl of dNTPs, and 6.5 µl of enzymes. 5.8 µl of this reaction mixture was added to each sample along with 14.2 µl of RNA and water based on the concentration of the samples to create a total of 20 µl solution per sample as shown in Table 1 below. These were briefly vortexes and centrifuged for 1 minute. Then, the samples were used to perform qPCR on a 96-well plate with the following primers: MT-CO1, D-Loop 1, D-Loop 3, and Beta-Actin. The reaction mixture for each primer was made using 140 µl

of SyBr Green, 14 µl of Forward Primer, and 14 µl of Reverse Primer. To create the PCR plate, 8 samples were used (Q7 Control, Q7 5 µM, Q7 10 µM, Q7 5 µM GA100, Q111 Control, Q111 5 µM, Q111 10 µM, Q111 5 µM GA100) and 3 wells were assigned for each sample and primer (3 replicates). 100 µl of Nuclease-free water was added to each cDNA tube and this was centrifuged for 2 minutes. From each sample reaction mixture prepared earlier, 6 µl was added to each well. 4 µl of the RNA sample was added in the well for a total of 10 µl per well. The plate was then centrifuged for 2 minutes and put in qPCR machine Quantstudio 3 from Thermo.

DNA Isolation and qPCR: DNA samples were isolated using the DNeasy Blood and Tissue Kit from QIAGEN. To collect DNA samples, cells were detached from the plate using trypsin, the solution was centrifuged (800 rpm) for 5 minutes, the cell pellet was dissolved in 200 µl of PBS, and then 200 µl of AL buffer, transferred into a 1.5 mL microcentrifuge tube and stored in -80°C freezer. DNA quantification data was collected using the Nanodrop 1000. Then, the samples were used to perform qPCR using the same method as mentioned above on a 96-well plate with the following primers: MT-CO1, D-Loop 1, D-Loop 3, and Beta-Actin. The reaction mixture for each primer was made using 140 µl of SyBr Green, 14 µl of Forward Primer, and 14 µl of Reverse Primer. 4 µl of sample DNA and 6 µl of reaction mixture was pipetted into each well.
Again, the same samples were used with 3 replicates per treatment and primer group. The plate was then centrifuged for 2 minutes and put in qPCR machine to collect data.

Table 1: RNA -> cDNA sample preparation

Sample	ng/mL	RNA	Water
Q7 Control	473.6	0.57	13.03
Q7 10 µM BC1618	24.7	11.04	3.16
Q7 10 µM GA100	19.2	14.2	0
Q111 Control	227.1	1.20	12.99
Q111 10 µM BC1618	37.3	7.30	6.89
Q111 10 µM GA100	62.6	4.36	9.84

Results

In this set of experiments, Q7 and Q111 were treated with two different compounds and collected protein, mRNA, and DNA for analysis.

Table 2: Protein Quantification from Bradford Assay

Sample	ng/µl Set 1	ng/µl Set 2
Q7 Control	0.929803	0.882702
Q7 5 µM BC1618		0.591375
Q7 10 µM BC1618	0.228526	1.276952
Q7 5 µM GA100		1.936362
Q7 10 µM GA100	0.151769	0.273882
Q111 Control	0.703021	0.572186
Q111 5 µM BC1618		0.736166
Q111 10 µM BC1618	0.694299	0.525085
Q111 5 µM GA100		0.990859
Q111 10 µM GA100	0.331449	0.275626

After collection of lysates for the protein as described in method, the lysates were quantified to determine the protein concentration using a Bradford assay. Although equal numbers of cells were plated per well, in the first assay I found that some lysates obtained from treated cells had significantly less protein than the untreated controls. This suggests that either there were technical errors or that the drugs were toxic. As a result, in the second repeat of this assay, I performed the experiment at multiple concentrations to determine if a nontoxic dose could be found. For GA100, the 5 µM appears to be less toxic than the 10 µM dose; data with BC1618 were more variable. Although I did not have time to run immunoblots on these samples, these lysates are in storage.

Table 3: RNA Quantification

Sample	ng/µl Set 1	260/280 Set 1	260/230 Set 1	ng/µl Set 2	260/280 Set 2	260/230 Set 2
Q7 Control	653.4	2.16	1.46	527.2	2.12	2.2
Q7 10 µM BC1618	46.6	2	1.51	3.1	2	0.39
Q7 10 µM GA100	126.4	2.13	2.02	27.9	2.19	0.21
Q111 Control	633	2.15	2.03	659.9	2.14	2.14
Q111 10 µM BC1618	91.6	2.15	1.33	2.8	1.11	0.5
Q111 10 µM GA100	58.4	2.12	0.51	5.2	1.36	0.49

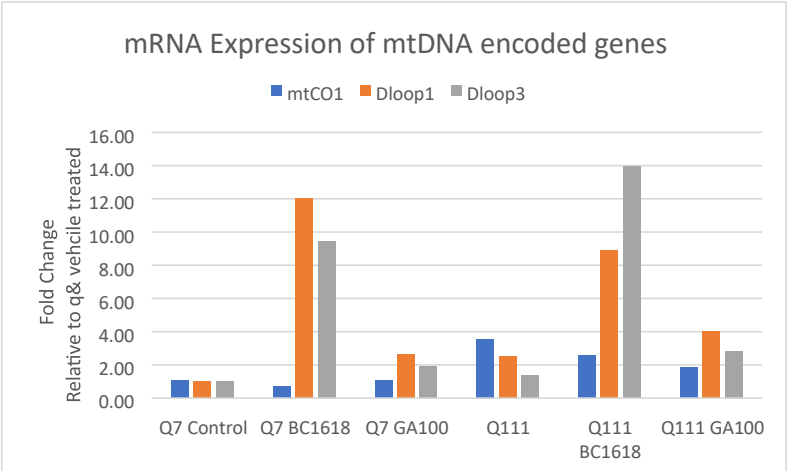

Figure 1: Analysis of Mitochondrial RNA Expression. Expression of mitochondrial mRNAs mtCO1, Dloop1, and DLoop 3 were quantified using qPCR followed by ΔΔCt analysis. N=1.

In addition to collecting protein, I also collected mRNA from treated cells for future gene expression analysis. I analyzed the quantity and quality of the mRNA collected. The concentration of RNA was obtained using A260 value. The quality of the RNA was assessed by looking at the A260/280 ratio (reference value >2.0) and the A260/320 ratio (reference value >2.0). These RNA samples were then used for qPCR analysis of gene expression.

RNA analysis shows that BC1618 and GA100 both increased the levels of mitochondrial mRNA genes mtCO1, Dloop1, and Dloop3, with the greatest increase in both Q7 and Q111 cells with BC1618 (Figure 1). Two possible explanations for this are increased expression of the mitochondrial genes in each mitochondrion or an increase in the number of mitochondria per cell. Thus, we analyzed mitochondrial DNA as an indicator of the number of mitochondria.

Table 4: DNA Quantification (Sets 1 and 2)

Sample	ng/µl Set 1	260/280 Set 1	260/230 Set 1	ng/µl Set 2	260/280 Set 2	260/230 Set 2
Q7 Control	991.5	2.12	2.11	1201.4	2.14	2.17
Q7 10 µM BC1618	29.1	1.93	0.99	190.4	2.12	1.89
Q7 10 µM GA100	2.2	1.41	0.44	5.3	1.95	0.22
Q111 Control	472.3	2.04	2.03	993.9	2.1	2.16
Q111 10 µM BC1618	72.5	2.12	1.67	344.1	2.07	2.01
Q111 10 µM GA100	6.4	1.96	0.4	24.2	1.95	0.81

Table 5: DNA Quantification (Sets 3 and 4)

Sample	ng/µl Set 3	260/280 Set 3	260/230 Set 3	ng/µl Set 4	260/280 Set 4	260/230 Set 4
Q7 Control	510.1	2.16	1.89	617.4	2.17	2.25
Q7 5 µM BC1618	569.9	2.13	1.89	508.1	2.14	2.07
Q7 10 µM BC1618	300.3	2.22	1.74	203	2.18	1.97
Q7 5 µM GA100	146.8	2.4	1.68	624.9	2.18	2.11
Q7 10 µM GA100	3.3	1.22	0.07	11.3	2.18	2.26
Q111 Control	849.3	2.18	1.97	69.6	2.23	1.31
Q111 5 µM BC1618	723.6	2.18	2.03	70.4	2.35	0.36
Q111 10 µM BC1618	577.7	2.13	2.05	55.2	2.23	1.04
Q111 5 µM GA100	876.7	2.2	1.98	665.2	2.22	2.23
Q111 10 µM GA100	18.2	2.08	0.55	6.4	1.83	0.64

Similarly, I collected DNA from treated and control samples. I analyzed the quantity and quality of the DNA collected. The concentration of DNA was obtained using A260 value. The quality of the RNA was assessed by looking at the A260/280 ratio (reference value >1.8) and the

A260/320 ratio (reference value >2.0). These DNA samples were then used for qPCR analysis of to determine mitochondrial biomass in the treated cells as compared with controls.

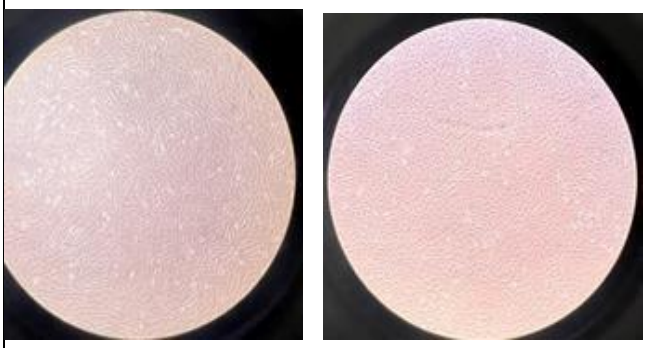

Figure 2: Q7 Control Cells (Left) and Q111 Control (Right). Cells when fully confluent shown under 10x magnification.

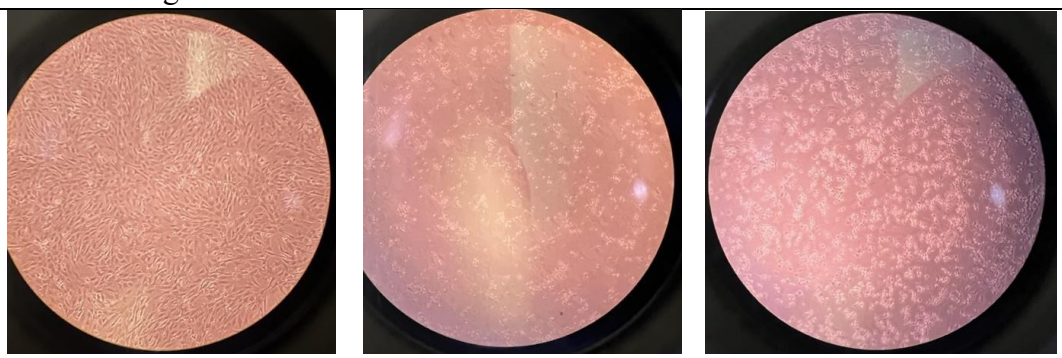

Figure 3: Q7 cells after treatment. Q7 Control (Left) is very confluent and growing well, Q7 BC1618 (Middle) shows significant decrease in cell size and growth, Q7 GA100 (Right) also shows reduced growth and cell size compared to Control.

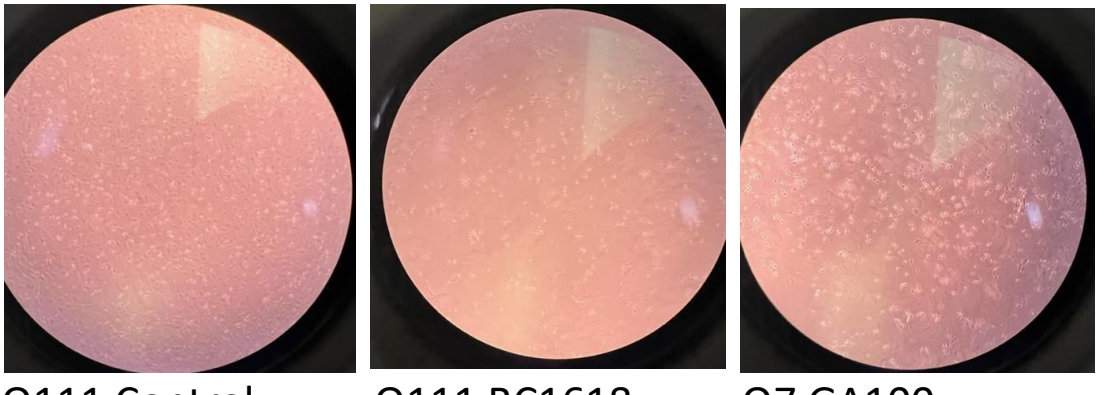

Figure 4. Q111 cells after treatment. Q111 Control (Left), Q111 BC1618 (Middle), Q111 GA100 (Right). Cell size and growth decreased after treatments, similar to Q7 cells.

In addition to objective measures of protein, RNA, and DNA quantity, I also recorded qualitative changes in cell density. I found that after treatment, there were fewer cells observed in both BC1618 and GA100 treated wells than in untreated controls (Figures 2-4). This confirms the hypothesis that treatment is either toxic to the cells or it prevents cell proliferation. In either case, the lower concentrations of cellular macromolecules that were found are likely due to the decreased number of cells found in treated wells.

Interestingly, although drug treatment decreased the number of cells per well, qPCR analysis of mitochondrial DNA showed an increase in the proportion of mitochondrial DNA (Figure 5). This suggests increased mitochondrial biomass in treated cells.

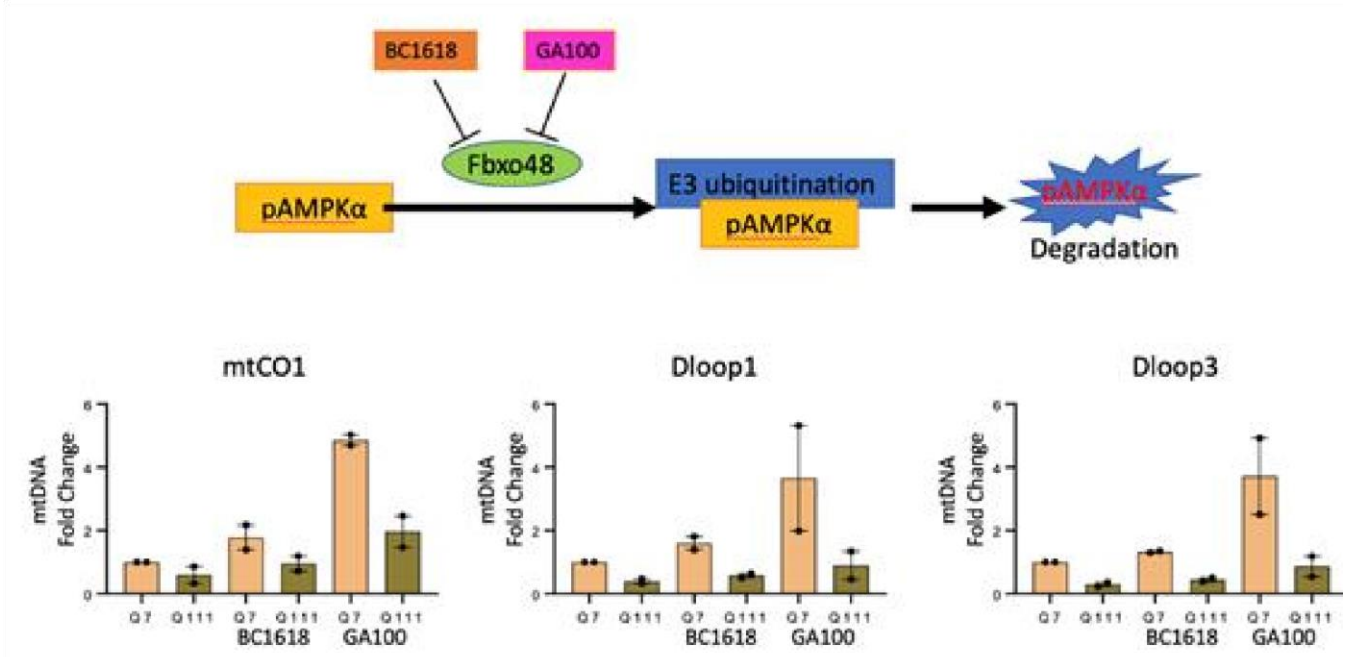

Figure 5: Regulation of mtDNA copy number in Q7 and Q111 cells by regulating pAMPKα degradation. Analysis of Mitochondrial Copy Number using qPCR. Expression of mitochondrial DNA using primers for mtCO1, Dloop1, and DLoop 3 were quantified using qPCR followed by ΔΔCt analysis. N=2.

Discussion

From viewing the cells under the microscope, it appears that BC1618 and GA100 treatments have resulted in decreased cell growth and size in both Q7 and Q111 cells. BC1618 shows a more significant decrease when compared to GA100 as can be seen in Figures 2 and 3.

As for the protein samples, the Western blot testing was inconclusive and would need to be repeated. Based on the most significant results obtained through this project were based on the qPCR testing of the DNA samples. As shown in Figure 4, qPCR results indicated that both BC1618 and GA100 caused increased fold change in the mitochondrial RNA, which could be caused by either increased transcription of the measured genes or by increased number of mitochondria per cell. The follow up analysis of mitochondrial DNA in both Q7 and Q111 cells showed that the mRNA increase is likely caused by increased number of mitochondria per cell. In reference to Figure 5, we can understand that BC1618 and GA100 are working by inhibiting

the interaction between the E3 ubiquitin ligase complex and the α subunit of Ampk, prolonging the activation of Ampk. This aligns with prior research which has found that AMPK protection slowed down the neurodegenerative effects of mHtt and demonstrates the therapeutic potential of Ampk-activation to treat HD (12). The findings are also consistent with previous studies which have shown that inhibiting Fbxo48 would prevent pAmpk degradation (4).

This experiment had some limitations which could be improved in the future to provide even better findings. One discrepancy was that only the 10 μM concentration of the treatments was initially used, however the 10 μM GA100 treatment showed little cell viability. This implies that this dosage may have been toxic to the cells. This would need to be investigated further by performing a cytotoxicity assay. Despite this finding, a second concentration level at 5 μM was then included in the treatment conditions, and this concentration of GA100 did not suggest toxicity. Additionally, the cell counts which were used when plating for the experiments was initially 1.5×10^6 cells per each culture dish. However, this count was doubled to 3.0×10^6 cells in order ensure that there were enough materials after collection for analysis, which would make any effects to be observed clearer. Finally, because some optimization experiments did not produce useable data due to the low number of surviving cells after treatment, the final N of the experiments was less than 3. Thus, all experiments need to be repeated. Nonetheless, the results that were obtained are promising.

In the future, obtaining more extensive data from Western blots and other assays may provide a more complete understanding of the impact of BC1618 and GA100 treatments. It may also be useful to test these treatments in both *in vivo* and *in vitro* models to assess the applicability of these treatments to live models and as potential treatments for humans.

References

1. Roos RA. Huntington's disease: a clinical review. Orphanet journal of rare diseases. 2010;5(1):40. https://doi.org/10.1186/1750-1172-5-40. PubMed PMID: 21171977; PMCID: 3022767.
2. Hervas D, Fornes-Ferrer V, Gomez-Escribano AP, Sequedo MD, Peiro C, Millan JM, VazquezManrique RP. Metformin intake associates with better cognitive function in patients with Huntington's disease. PLoS One. 2017;12(6):e0179283. Epub 2017/06/21. https://doi.org/10.1371/journal.pone.0179283. PubMed PMID: 28632780; PMCID: PMC5478119.
3. Sanchis A, Garcia-Gimeno MA, Canada-Martinez AJ, Sequedo MD, Millan JM, Sanz P, VazquezManrique RP. Metformin treatment reduces motor and neuropsychiatric phenotypes in the zQ175 mouse model of Huntington disease. Experimental & molecular medicine. 2019;51(6):1-16. Epub 2019/06/06. https://doi.org/10.1038/s12276-019-0264-9. PubMed PMID: 31165723; PMCID: PMC6549163.
4. Liu Y, Jurczak MJ, Lear TB, Lin B, Larsen MB, Kennerdell JR, Chen Y, Huckestein BR, Nguyen MK, Tuncer F, Jiang Y, Monga SP, O'Donnell CP, Finkel T, Chen BB, Mallampalli RK. A Fbxo48 inhibitor prevents pAMPKalpha degradation and ameliorates insulin resistance. Nat Chem Biol. 2021;17(3):298-306. Epub 2021/01/27. https://doi.org/PubMed PMID: 33495648; PMCID: PMC8529588.
5. Trettel F, Rigamonti D, Hilditch-Maguire P, Wheeler VC, Sharp AH, Persichetti F, Cattaneo E, MacDonald ME. Dominant phenotypes produced by the HD mutation in STHdh(Q111) striatal cells. Hum Mol Genet. 2000;9(19):2799-809. PubMed PMID: 11092756.
6. Milakovic T, Johnson GV. Mitochondrial respiration and ATP production are significantly impaired in striatal cells expressing mutant huntingtin. J Biol Chem. 2005;280(35):30773-82. https://doi.org/10.1074/jbc.M504749200. PubMed PMID: 15983033.
7. Yano H, Baranov SV, Baranova OV, Kim J, Pan Y, Yablonska S, Carlisle DL, Ferrante RJ, Kim AH, Friedlander RM. Inhibition of mitochondrial protein import by mutant huntingtin. Nat Neurosci. 2014;17(6):822-31. https://doi.org/10.1038/nn.3721. PubMed PMID: 24836077.
8. Jauhari A, Baranov SV, Suofu Y, Kim J, Singh T, Yablonska S, Li F, Wang X, Oberly P, Minnigh MB, Poloyac SM, Carlisle DL, Friedlander RM. Melatonin inhibits cytosolic mitochondrial DNA-induced neuroinflammatory signaling in accelerated aging and neurodegeneration. J Clin Invest. 2020. Epub 2020/03/18. https://doi.org/10.1172/JCI135026. PubMed PMID: 32182222.
9. Livak KJ, Schmittgen TD. Analysis of relative gene expression data using real-time quantitative PCR and the 2(-Delta Delta C(T)) Method. Methods. 2001;25(4):402-8. https://doi.org/10.1006/meth.2001.1262. PubMed PMID: 11846609.
10. Suofu Y, Li W, Jean-Alphonse FG, Jia J, Khattar NK, Li J, Baranov SV, Leronni D, Mihalik AC, He Y, Cecon E, Wehbi VL, Kim J, Heath BE, Baranova OV, Wang X, Gable MJ, Kretz ES, Di Benedetto G, Lezon TR, Ferrando LM, Larkin TM, Sullivan M, Yablonska S, Wang J, Minnigh MB, Guillaumet G, Suzenet F, Richardson RM, Poloyac SM, Stolz DB, Jockers R, Witt-Enderby PA, Carlisle DL, Vilardaga JP, Friedlander RM. Dual role of mitochondria in producing melatonin and driving GPCR signaling to block cytochrome c release. Proc Natl Acad Sci U S A. 2017;114(38):E7997-E8006. https://doi.org/10.1073/pnas.1705768114. PubMed PMID: 28874589; PMCID: PMC5617277.

11. Baranov SV, Baranova OV, Yablonska S, Suofu Y, Vazquez AL, Kozai TDY, Cui XT, Ferrando LM, Larkin TM, Tyurina YY, Kagan VE, Carlisle DL, Kristal BS, Friedlander RM. Mitochondria modulate programmed neuritic retraction. Proc Natl Acad Sci U S A. 2019; 116(2):650-9. Epub 2018/12/26. https://doi.org/10.1073/pnas. 1811021116. PubMed PMID: 30584104; PMCID: PMC6329959.
12. Vázquez-Manrique, R. P., Farina, F., Cambon, K., Dolores Sequedo, M., Parker, A. J., Millán, J. M., Weiss, A., Déglon, N., & Neri, C. (2016). AMPK activation protects from neuronal dysfunction and vulnerability across nematode, cellular and mouse models of Huntington's disease. Human molecular genetics, 25(6), 1043–1058. https://doi.org/10.1093/hmg/ddv513
13. Trujillo-Del Río, C., Tortajada-Pérez, J., Gómez-Escribano, A. P., Casterá, F., Peiró, C., Millán, J. M., Herrero, M. J., & Vázquez-Manrique, R. P. (2022). Metformin to treat Huntington disease: A pleiotropic drug against a multi-system disorder. Mechanisms of Ageing and Development, 204, 111670. https://doi.org/10.1016/j.mad.2022.111670
14. Ferguson, M. W., Kennedy, C. J., Palpagama, T. H., Waldvogel, H. J., Faull, R. L. M., & Kwakowsky, A. (2022). Current and Possible Future Therapeutic Options for Huntington's Disease. Journal of central nervous system disease, 14, 11795735221092517. https://doi.org/10.1177/11795735221092517